Molecular Cancer Therapeutics

IMGN853, a Folate Receptor-α (FRα)–Targeting Antibody–Drug Conjugate, Exhibits Potent Targeted Antitumor Activity against FRα-Expressing Tumors

Olga Ab[1], Kathleen R. Whiteman[2], Laura M. Bartle[1], Xiuxia Sun[3], Rajeeva Singh[3], Daniel Tavares[4], Alyssa LaBelle[5], Gillian Payne[6], Robert J. Lutz[7], Jan Pinkas[2], Victor S. Goldmacher[1], Thomas Chittenden[8], and John M. Lambert[8]

Abstract

A majority of ovarian and non–small cell lung adenocarcinoma cancers overexpress folate receptor α (FRα). Here, we report the development of an anti-FRα antibody–drug conjugate (ADC), consisting of a FRα-binding antibody attached to a highly potent maytansinoid that induces cell-cycle arrest and cell death by targeting microtubules. From screening a large panel of anti-FRα monoclonal antibodies, we selected the humanized antibody M9346A as the best antibody for targeted delivery of a maytansinoid payload into FRα-positive cells. We compared M9346A conjugates with various linker/maytansinoid combinations, and found that a conjugate, now denoted as IMGN853, with the *N*-succinimidyl 4-(2-pyridyldithio)-2-sulfobutanoate (sulfo-SPDB) linker and $N^{2'}$-deacetyl-$N^{2'}$-(4-mercapto-4-methyl-1-oxopentyl)-maytansine (DM4) exhibited the most potent antitumor activity in several FRα-expressing xenograft tumor models. The level of expression of FRα on the surface of cells was a major determinant in the sensitivity of tumor cells to the cytotoxic effect of the conjugate. Efficacy studies of IMGN853 in xenografts of ovarian cancer and non–small cell lung cancer cell lines and of a patient tumor-derived xenograft model demonstrated that the ADC was highly active against tumors that expressed FRα at levels similar to those found on a large fraction of ovarian and non-small cell lung cancer patient tumors, as assessed by immunohistochemistry. IMGN853 displayed cytotoxic activity against FRα-negative cells situated near FRα-positive cells (bystander cytotoxic activity), indicating its ability to eradicate tumors with heterogeneous expression of FRα. Together, these findings support the clinical development of IMGN853 as a novel targeted therapy for patients with FRα-expressing tumors. *Mol Cancer Ther; 14(7); 1605–13. ©2015 AACR.*

Introduction

The folate receptor-α (FRα) is a glycosylphosphatidylinositol-linked cell-surface glycoprotein that has high affinity for folates (1). Its physiologic role in normal and cancerous tissues has not yet been fully elucidated. Most normal tissues do not express FRα, and transport of physiologic folates into most cells is thought to be mediated by several other proteins, most notably, reduced folate carrier (2). High levels of FRα have been found in serous and endometrioid epithelial ovarian cancer, endometrial adenocarcinoma, and non–small cell lung cancer of the adenocarcinoma subtype (3–8). Importantly, FRα expression is maintained in metastatic foci and recurrent carcinomas in ovarian cancer patients (9), and after chemotherapy in epithelial ovarian and endometrial cancers (10). These properties, together with the highly restricted expression of FRα on normal tissues, make FRα a highly promising target for cancer therapy, and have prompted a variety of experimental approaches for developing FRα-targeted therapies (11–13).

Two FR-targeting agents with distinct mechanisms of action, vintafolide (EC145), which targets both FRα and FRβ, and farletuzumab, which is FRα-specific, have been evaluated in advanced-stage clinical trials. Vintafolide is a small-molecule conjugate of folate with a cytotoxic *vinca* alkaloid, which is selectively internalized into cells through binding and uptake by FRs (14, 15). Vintafolide showed promising clinical activity in a randomized phase II study in combination with pegylated liposomal doxorubicin for treatment of FR^+, platinum-resistant, ovarian cancer (16), but a phase III study failed to confirm the clinical benefit of vintafolide in this setting. The agent is under investigation as a therapy for other FR^+ tumors. EC1456, a conjugate of folic acid with a more potent than *vinca* alkaloid cytotoxic effector, tubulysin (17), demonstrated strong antitumor activity in human

[1]Department of Cell Biology, ImmunoGen, Inc., Waltham, Massachusetts. [2]Department of Pharmacology Toxicology, ImmunoGen, Inc., Waltham, Massachusetts. [3]Department of Biochemistry, ImmunoGen, Inc., Waltham, Massachusetts. [4]Department of Antibody Engineering, ImmunoGen, Inc., Waltham, Massachusetts. [5]Department of Biomarkers, ImmunoGen, Inc., Waltham, Massachusetts. [6]Department of Bioanalytical Science, ImmunoGen, Inc., Waltham, Massachusetts. [7]Department of Translational Research and Development, ImmunoGen, Inc., Waltham, Massachusetts. [8]Research and Development, ImmunoGen, Inc., Waltham, Massachusetts.

Note: Supplementary data for this article are available at Molecular Cancer Therapeutics Online (http://mct.aacrjournals.org/).

Current address for A. LaBelle: Pharmacology Department, Case Western Reserve University, Cleveland, Ohio.

Corresponding Author: Olga Ab, ImmunoGen, Inc., 830 Winter Street, Waltham, MA 02451. Phone: 781-895-0688; Fax: 781-895-0611; E-mail: olga.ab@immunogen.com

doi: 10.1158/1535-7163.MCT-14-1095

xenograft models (18), and recently entered a phase I study. Farletuzumab (MORAb-003), a humanized anti-FRα monoclonal antibody that was reported to exert antitumor activity through antibody-dependent cellular cytotoxicity and complement-dependent cytotoxicity (19), has been evaluated in ovarian cancer patients as a single agent, and in combination with chemotherapy. A phase III study that tested farletuzumab in combination with carboplatin and a taxane did not meet its primary endpoint of improved progression-free survival in platinum-sensitive ovarian cancer patients (20). A second phase III trial evaluated farletuzumab in platinum-resistant ovarian cancer patients in combination with paclitaxel, but was stopped early after failing an interim futility analysis. Therapy with this FRα-targeting nonconjugated antibody was generally well tolerated, but to date has not been proven to be efficacious. Thus, emerging clinical data indicate that there is a need for FRα-targeted agents with improved antitumor activity.

Antibody–drug conjugates (ADC) composed of highly cytotoxic agents conjugated to antibodies that bind to tumor-associated antigens represent a promising therapeutic strategy to enhance the potency of tumor-targeting antibodies. ADCs offer the potential to combine the favorable pharmacokinetics, biodistribution, and tumor-targeting properties of antibodies with the potent cell killing mechanism provided by the attached small molecule, or payload. Clinical validation of this concept has been achieved with the regulatory approval of two ADCs, brentuximab vedotin for relapsed/refractory Hodgkin disease and anaplastic large cell lymphoma and ado-trastuzumab emtansine for recurrent human epidermal growth factor receptor 2 (Her2)–positive breast cancer (21–24). The latter conjugate consists of the HER2-targeting antibody, trastuzumab, conjugated by the thioether linker, SMCC, to the maytansinoid, DM1. Maytansinoids are microtubule-targeting heterocyclic compounds that induce mitotic arrest and subsequent cell death (25, 26). Promising results have been reported with a number of additional antibody–maytansinoid conjugates in earlier stages of clinical development (27–30).

Here, we describe the preclinical development of a FRα-targeting antibody–maytansinoid conjugate, IMGN853. The design of this FRα-targeting ADC, including selection of its antibody and linker components, was based on optimization of its antitumor activity. IMGN853 exhibited potent anticancer activity that was dependent on the expression of FRα. Moreover, IMGN853 was highly active in tumor models having levels of FRα expression representative of those in tumor samples from patients with ovarian and non-small cell lung cancer, supporting the development of this ADC as a novel FRα-targeted therapy.

Materials and Methods

Cell lines

KB (human cervical adenocarcinoma), Jeg-3 (human choriocarcinoma), Skov-3, Ovcar-3 and Ov-90 (human ovarian adenocarcinomas), and HCC827 and H2110 (human lung adenocarcinomas) were purchased from the ATCC. Igrov-1 human ovarian carcinoma was purchased from the Division of Cancer Treatment and Diagnostics, the National Cancer Institute, Frederick, Maryland. Ishikawa human endometrial adenocarcinoma was purchased from the European Collection of Cell Cultures. The cell lines were obtained within the period of 2000–2015. The cell lines were characterized by the manufacturers; no further cell line authentication was conducted. Upon receiving from a manufacturer, each cell line was expanded by passaging two to three times, aliquoted, and frozen. For use in experiments, cell lines were cultured in media recommended by the manufacturers in a humidified incubator at 37°C, 6% CO_2 for no longer than 2 months.

Immunoconjugates

Anti-FRα ADCs were prepared with either $N^{2'}$-deacetyl-$N^{2'}$-(3-mercapto-1-oxopropyl)-maytansine (DM1) or $N^{2'}$-deacetyl-$N^{2'}$-(4-mercapto-4-methyl-1-oxopentyl)-maytansine (DM4) via the succinimidyl-4-(*N*-maleimidomethyl)cyclohexane-1-carboxylate (SMCC), the *N*-succinimidyl 4-(2-pyridyldithio)pentanoate (SPP), the *N*-succinimidyl 4-(2-pyridyldithio)butanoate (SPDB), or the *N*-succinimidyl 4-(2-pyridyldithio)-2-sulfobutanoate (sulfo-SPDB) linkers according to the protocols developed at ImmunoGen, Inc. and described previously (31–33). The maytansinoid per antibody ratio varied from 3.3 to 5.0.

Immunohistochemistry

Immunohistochemical (IHC) staining of FRα in formalin-fixed paraffin-embedded cell lines, normal and tumor tissues, and human xenograft tissues were performed using anti-FRα antibody clone BN3.2 and the Leica Bond RX Automated Stainer (both purchased from Leica Microsystems). Slides were baked at 60°C and dewaxed using Bond Dewax Solution (Leica Biosystems) and absolute ethanol. Following a 20-minute heat-induced epitope retrieval using Bond Epitope Retrieval 2 (ethylenediaminetetraacetic acid–based solution, pH 9.0; Leica Biosystems) and a 5-minute treatment with 3% hydrogen peroxide to inactivate endogenous peroxidase, slides were incubated with either the anti-FRα murine monoclonal antibody BN3.2, or an isotype-control antibody (muIgG1; Beckman Coulter) at 1.9 μg/mL for 15 minutes, developed using Bond Refine detection system (Leica Biosystems) and counterstained with hematoxylin. All tissue slides were evaluated and scored by a board-certified pathologist. FRα staining intensity was scored on a scale of 0 to 3 (0 = no specific staining similar to that of the isotype control, 1 = weak, 2 = moderate, and 3 = strong staining). Uniformity of the staining was scored as negative (no cells exhibited positive staining), focal (<25% of cells stained), heterogeneous (25%–75% of cells stained), and homogeneous (>75% of cells stained).

Generation of anti-FRα monoclonal antibodies

Balb/c mice were immunized with either FRα-positive KB cells, or the murine syngeneic B cell line 300-19 stably transfected with human FRα. The hybridoma clones were produced as described previously (34) and screened by flow cytometry with FRα-positive and -negative cell lines for secretion of anti-FRα antibodies. Antibodies were purified using MabSelect SuRe (Amersham Biosciences) in accordance with the manufacturer's protocol.

Binding assay

Binding of anti-FRα antibodies and their maytansinoid conjugates to cells was evaluated flow-cytometrically by indirect immunofluorescence. Briefly, 2×10^4 cells per well in a 96-well plate were incubated for 2 hours at 4°C with an anti-FRα antibody diluted to various concentrations in assay medium [RPMI-1640 supplemented with 2% (*w*/*v*) bovine serum albumin (Sigma)]. The cells were than washed with the cold assay medium, stained with fluorescein isothiocyanate–labeled goat anti-murine or anti-human immunoglobulin G (IgG) antibody for 40 minutes at 4°C

in the dark, washed with the cold assay medium, fixed in a solution of phosphate-buffered saline, pH 7.4 (PBS) containing 1% formaldehyde, and analyzed using a FACSCalibur flow cytometer (BD Bioscience). The concentration of the antibody achieving half-maximal binding was taken as the apparent affinity (K_d) of the antibody.

Indirect ("piggyback") cytotoxicity assay

Fab-fragment of polyclonal anti-murine antibody (Jackson ImmunoResearch Laboratories) conjugated to DM4 via a non-reducible linker was used. In initial sets of experiments, cells were exposed to a range of Fab-DM4 concentrations, and the maximal nontoxic concentration of the conjugate was chosen. The concentration varied from 0.1 to 1 nmol/L depending on the cell line. Serial dilutions of anti-FRα antibodies in culture medium that contained the maximal nontoxic concentration of Fab-DM4 were added to cells (1×10^3/well to reach a total volume of 200 μL/well). The plates were incubated for 5 days at 37°C, 6% CO_2. Cell viability was determined by the WST-8 assay (Donjindo Molecular Technologies, Inc.) in accordance with the manufacturer's protocol. Later, we confirmed that the ranking of the cytotoxic activities of the available anti-FRα antibody–maytansinoid conjugates *in vitro* was reliably predicted by the ranking of the cytotoxic activities of the respective antibodies in the indirect assay.

Cytotoxicity assay

Dilutions of conjugates or unconjugated maytansinoid in the appropriate culture medium were added to wells of 96-well flat-bottomed plates containing 1×10^3 cells per well. The plates were incubated at 37°C, 6% CO_2 for either 5 days (continuos exposure) or for 4 hours followed by 5-day incubation in conjugate-free medium (short exposure). Cell viability was determined by the WST-8 assay (Donjindo Molecular Technologies, Inc.) in accordance with the manufacturer's protocol, and IC_{50} were generated using a sigmoidal dose–response (variable slope) nonlinear regression curve fit (GraphPad Software Inc.).

IMGN853 processing

To identify maytansinoid catabolites of IMGN853 formed within FRα-positive cancer cells, KB cells were treated with ^{3}[H]-IMGN853 for 30 minutes, and ^{3}[H]-labeled metabolites were analyzed after 22-hour incubation in ^{3}[H]-IMGN853-free medium by HPLC and liquid scintillation counting. The detailed protocol was reported previously (35). To analyze IMGN853 processing by various FRα-positive cell lines, cells were exposed to 25 nmol/L (a saturating concentration) of ^{3}[H]-IMGN853 or ^{3}[H]-M9346A for 30 minutes at 37°C, washed in PBS to remove any unbound antibody or conjugate, resuspended in fresh culture medium, and incubated at 37°C in a humidified 6% CO_2 atmosphere for 22 hours. The amount of protein-free radioactivity (processed antibody) and protein-associated radioactivity (unprocessed antibody) was assessed following acetone extraction and liquid scintillation counting, and the data were used to calculate the antibody-binding sites per cell (ABC), % processed antibody, and pmol processed antibody (see the detailed description in Supplementary Methods).

Bystander cytotoxic activity

A mixed culture of FRα-positive cells 300-19 transfected with human FRα (FRα-300-19) and FRα-negative cells 300-19 was exposed to IMGN853 at a concentration that is nontoxic for the FRα-negative cells but highly toxic for the receptor-positive cells (killing 100% of the cells). Cells were incubated for 4 days, and the inhibition of cell proliferation was determined by WST-8-based assay (Dojindo Molecular Technologies).

***In vivo* efficacy**

Five-week-old female CB-17 severe combined immunodeficient (SCID) mice were obtained from Charles River Laboratories and quarantined for 7 days prior to study initiation. Mice were inoculated subcutaneously with cells (1×10^7 cells per mouse) resuspended in serum-free culture media (KB, Igrov-1 cells) or 50% Matrigel in serum-free culture media (Ovcar-3, Skov-3, Ov-9, and H2110 cells). When tumor volume reached about 130 mm^3, mice were randomized and received a single intravenous bolus injection of PBS (control) or maytansinoid conjugates. Tumor dimensions were measured two or three times per week and volume was calculated as $^1/_2$ ($L \times W \times H$), where L is the length, W is the width, and H is the height of the tumor. All procedures were carried out in accordance with the "Guide for the Care and Use of Laboratory Animals" (National Research Council).

Efficacy studies on a patient-derived non-small cell lung cancer xenograft model LXFA-737 were performed at Oncotest GmbH. Female NMRI nu/nu mice, 6-weeks old, were obtained from Harlan Laboratories. LXFA-737 tumor xenografts were serially passaged in nude mice. After removal from donor mice, tumors were cut into fragments (4–5 mm diameter) and transplanted into recipient mice. After tumor size reached about 110 mm^3, mice received a single intravenous injection of a maytansinoid conjugate or PBS. Tumor dimensions were measured twice weekly and volume was calculated as ($A \times B^2$) × 0.5, where A represents the largest and B the perpendicular tumor diameter. All experiments were conducted according to the guidelines of the German Animal Welfare Act (Tierschutzgesetz).

Typically, 6 mice per group were used. A partial tumor regression was defined as a reduction in tumor volume by 50% or greater. A complete tumor regression was scored when no palpable tumor could be detected.

A two-tailed Student t test was used to test the null hypotheses that there are no statistical significance differences in tumor volumes of mice that underwent various treatments. No adjustments for multiplicity were attempted and all tests were carried out at the 0.05 α level.

Results

Selection of a FRα-binding antibody for a maytansinoid ADC

The overexpression of FRα in various malignancies makes it an attractive target for ADC development. Because no clear functional role has been established for FRα in tumor cell growth or survival (36), we sought to identify the optimal antibody component for a FRα-targeting ADC based on its ability to deliver a maytansinoid payload to FRα-expressing tumors *in vitro* and *in vivo*. An additional antibody selection criterion was equivalent binding to both human and monkey FRα, in order to enable relevant preclinical toxicology studies.

A panel of murine monoclonal FRα-binding antibodies was generated by standard hybridoma procedures and screened for binding by flow cytometry to cell lines expressing either human or monkey FRα. Antibodies were screened for their capacity to deliver a maytansinoid payload into FRα-positive cells using a high-throughput indirect "piggyback" cytotoxicity assay. In this

assay, cells were exposed to a mixture of an anti-FRα antibody and a goat anti-murine-IgG polyclonal antibody Fab fragment conjugated to the maytansinoid DM4. Fab format was used for the secondary ADC rather than whole IgG to avoid possible cross-linking of FRα by the secondary ADC, which might affect the cytotoxicity of the complex. More than a hundred anti-FRα antibodies were tested and found to widely differ in their piggyback cytotoxic potencies (summarized in Supplementary Fig. S1). A subset of the most active murine antibodies identified by this indirect ADC cytotoxicity assay were evaluated as direct maytansinoid conjugates *in vitro* and five of these were then selected for humanization. In addition, a humanized derivative of the previously described anti-FRα antibody Mov19 (4, 37, 38), denoted M9346A, was prepared and added to the group of antibodies to be evaluated. The antibodies were humanized by variable domain resurfacing (39).

To compare the ability of the selected antibodies to deliver a cytotoxic payload, a noncleavable linker was chosen over a cleavable linker. This was done to avoid bystander cytotoxic activity of cleavable conjugates that could contribute to their *in vitro* and *in vivo* activity. Inside the cell, reducible maytansinoid conjugates are processed and release cytotoxic metabolites that cross cellular membranes and kill neighboring cells (bystander cytotoxic activity), while the metabolites released after processing of nonreducible conjugates do not easily penetrate cellular membranes (40). Results of representative comparative studies for five of the conjugates using the FRα-positive KB cell line are shown in Table 1 for *in vitro* binding and cytotoxicity, and in Fig. 1 and Supplementary Table S1 for *in vivo* efficacy. Although these conjugates were similar in their affinity toward FRα and in their cytotoxic potency *in vitro*, the conjugate of the M9346A antibody was significantly more active *in vivo*, as supported by the results of the Student *t* test, Supplementary Tables S2A and S2B. In similar comparative *in vivo* experiments, the M9346A antibody invariably yielded the most active conjugate and therefore was chosen as the most promising antibody candidate for a maytansinoid ADC. To test whether the superior activity of the M9346A conjugate *in vivo* was related to an activity of its antibody moiety, we examined unconjugated M9346A antibody. *In vitro*, M9346A exhibited some antibody-dependent cell-mediated cytotoxicity against FRα-positive Igrov-1 cells (Supplementary Fig. S2), while no detectable complement-dependent cytotoxicity or anti-proliferative activity against target-positive cells was observed. *In vivo*, the M9346A antibody did not exhibit any antitumor activity against KB xenograft tumors (Supplementary Fig. S3). Although the basis for the superior *in vivo* efficacy of the M9346A conjugate has not been identified, varying *in vivo* efficacies of anti-CD22–SMCC–DM1 conjugates with similar affinity and *in vitro* potency has also been reported (41).

Table 1. Comparative *in vitro* characterization of SMCC-DM1 conjugates of five humanized anti-FRα monoclonal antibodies and a humanized nontargeting antibody

Anti-FRα antibody	K_d, nmol/L[a]	IC_{50}, nmol/L[b]
huFR1-48	0.19 ± 0.08	0.07 ± 0.02
huFR1-49	0.08 ± 0.07	0.07 ± 0.01
huFR1-57	0.18 ± 0.06	0.15 ± 0.02
huFR1-65	0.16 ± 0.07	0.08 ± 0.02
M9346A	0.08 ± 0.02	0.10 ± 0.02
Nontargeting Ab	There was no detectable binding at 10 nmol/L	There was no detectable cytotoxicity at 10 nmol/L

NOTE: Data represent the mean ± SD of three independent experiments.
[a]Apparent affinity, flow-cytometric binding assay on Skov-3 cells; the affinities of the conjugates were similar to the affinities of the respective antibodies.
[b]The cytotoxicities of anti-FRα-SMCC-DM1 conjugates for KB cells, five-day continuous exposure.

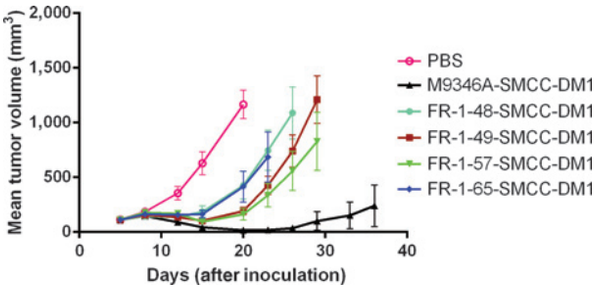

Figure 1.
In vivo activities of SMCC–DM1 conjugates of five humanized anti-FRα antibodies. Mice with established KB xenografts were dosed with a single intravenous injection of 200 μg of conjugated maytansinoid per kg, equivalent to 10 ± 2 mg/kg antibody on day 6 after cell inoculation. Some variability of the doses is the result of slightly different maytansinoid per antibody ratios of the tested conjugates. The exact doses for each group are listed in Supplementary Table S1. Mean tumor volumes in mm^3 versus time (in days) after cell inoculation are plotted. The Student *t* test of day 20 (postinoculation) data showed that the differences between tumor volumes in the sets of mice treated with any of the conjugates and vehicle control were statistically significant (Supplementary Table S2A), and that M9346A–SMCC–DM1 was significantly more active than any of the other four conjugates.

Optimization of the ADC linker/maytansinoid combination

Following selection of M9346A as the antibody component, further studies were conducted to optimize the design of an FRα-targeted ADC. Conjugates of M9346A with four linker/maytansinoid combinations, SPP-DM1 (hindered disulfide linker), SPDB-DM4 (highly hindered disulfide linker), sulfo-SPDB-DM4 (highly hindered disulfide hydrophilic linker), and a thioether-based SMCC-DM1 were prepared (depicted in Fig. 2A). These conjugates were tested for their cytotoxicity against three cell lines, KB, Igrov-1, and Jeg-3 (Table 2), which differed in the expression levels of FRα (Table 3). The conjugates were equally cytotoxic against KB cells, which had the highest FRα expression, while the disulfide-linked conjugates were more active than the thioether conjugate against the two cell lines with lower expression, Igrov-1 and Jeg-3. The cytotoxic activity of the conjugates was demonstrated to be FRα-selective because it decreased by at least 10-fold in the presence of a saturating excess of the M9346A antibody.

Having established that the four M9346A conjugates showed potent antigen-selective cytotoxicity *in vitro*, their efficacy against tumor xenograft models in immunodeficient mice was evaluated. M9346A–SMCC–DM1 conjugate was highly efficacious against the KB xenograft model at a dose of 11 mg/kg (Fig. 1), but only marginally active at a lower dose of 2.5 mg/kg (Fig. 2B). In contrast, the DM4-containing disulfide-linked conjugates were highly active at the 2.5 mg/kg dose level, with M9346A-sulfo-SPDB-DM4 being equally or more active than the other conjugates in all tested models (Fig. 2C–E), as supported by the Student *t* test analysis (Supplementary Tables S3–S5). The less hindered disulfide-containing SPP–DM1 conjugate was less active than the DM4-containing conjugates. A nontargeting isotype-matched antibody–SPDB–DM4 conjugate was inactive against KB model even at a 2-fold higher dose (5 mg/kg) demonstrating that the

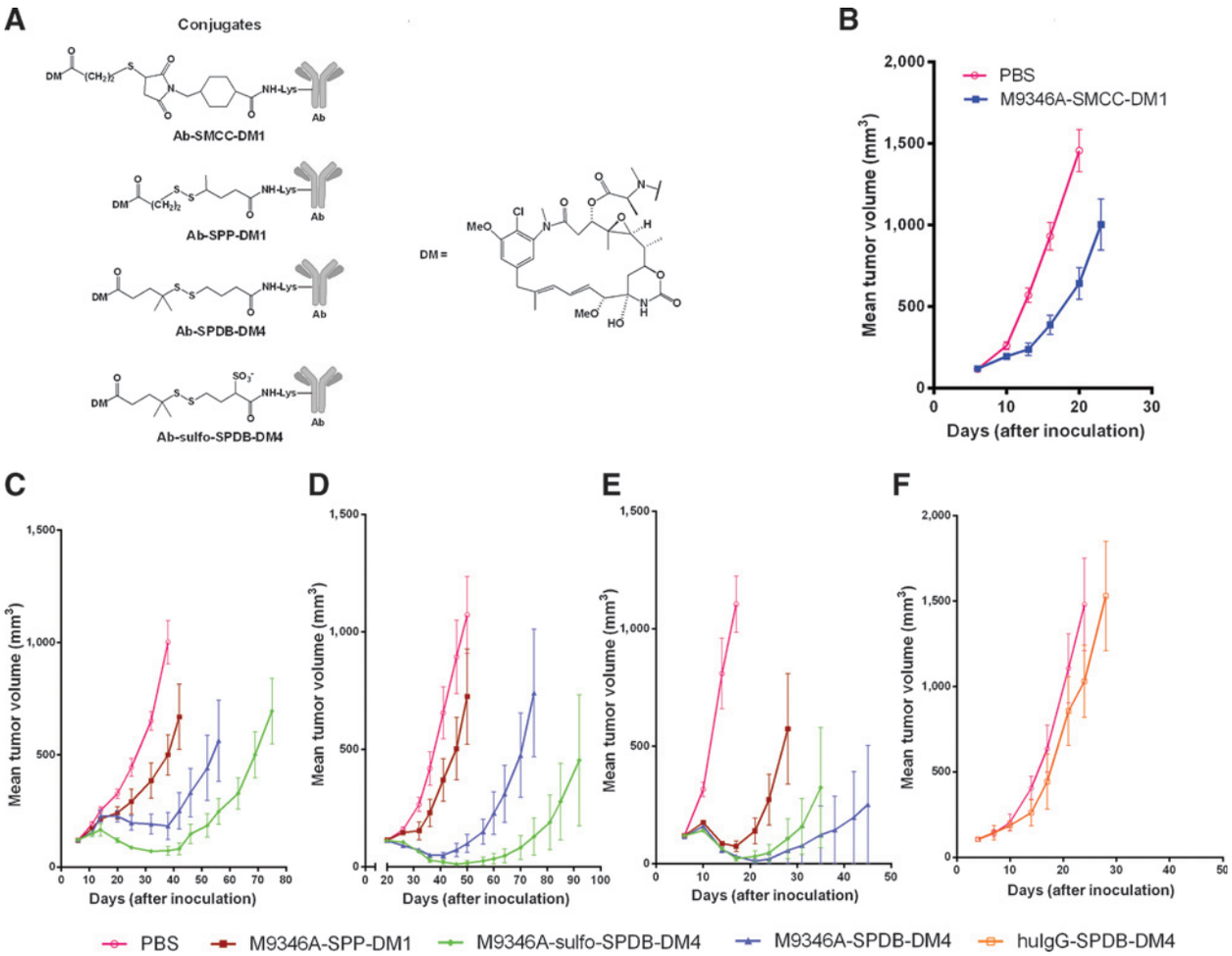

Figure 2.
Activity of M9346A noncleavable and cleavable maytansinoid conjugates *in vivo*. A, structure of the linker-maytansinoid moieties of the analyzed conjugates. B–F, activity of the thioether-based SMCC–DM1 conjugate against KB xenograft model (B), and three disulfide-linked conjugates against Igrov-1 (C), Ovcar-3 (D) and KB (E), and nontargeting disulfide-linked conjugate huIgG1–SPDB–DM4 against KB (F) xenograft models. Animals with established tumors of about 130 mm^3 were treated with intravenous single injection of the M9346A–DM conjugates at 2.5 ± 0.2 mg/kg, equivalent to 51 ± 3 μg conjugated maytansinoid per kg. The conjugates were injected on day 7 (B, C, and E), day 20 (D), or day 4 (F) after cell inoculation. Nontargeting huIgG1–SPDB–DM4 conjugate was administered at a 2-fold higher dose (5.0 mg/kg). Some variability of the doses is the result of slightly different maytansinoid per antibody ratios of the tested conjugates; the exact doses for each group are listed in Supplementary Table S1. Mean tumor volumes in mm^3 versus time (in days) after cell inoculation are plotted. Statistical analysis of the data is reported in Supplementary Tables S3–S5.

antitumor activity of M9346A conjugates was FRα-selective (Fig. 2F). On the basis of these data, M9346A-sulfo-SPDB-DM4 (denoted as IMGN853) was chosen for further examination.

IMGN853 exhibits bystander cytotoxic activity

Disulfide-linked maytansinoid ADCs have been shown to elicit bystander cytotoxic activity due to the formation of active maytansinoid metabolites that are able to diffuse from antigen-positive cancer cells into the neighboring cells (40). The bystander cytotoxic activity of IMGN853 was assessed using mixed cell culture assays of FRα-negative murine B cell line 300-19 and its subline transfected with human FRα. At 5 nmol/L, IMGN853 was not active against FRα-negative 300-19 cells in the absence of FRα-positive cells, but completely eradicated both positive and negative cancer cells in the mixed culture, demonstrating its bystander cytotoxic activity (Supplementary Fig. S4).

Table 2. The *in vitro* cytotoxic activity of M9346A conjugates with various linker/maytansinoid combinations

	IC_{50}, nmol/L (continuous exposure)			
Cells	**SPP-DM1**	**SPDB-DM4**	**Sulfo-SPDB-DM4**	**SMCC-DM1**
KB	0.11 ± 0.04	0.08 ± 0.01	0.15 ± 0.08	0.08 ± 0.01
Igrov-1	0.14 ± 0.05	0.07 ± 0.02	1.0 ± 0.4	2.0 ± 0.7
Jeg-3	0.13 ± 0.08	0.11 ± 0.08	0.2 ± 0.1	7.0 ± 2.0

NOTE: Data represent the mean ± SD of three independent experiments.

Table 3. M9346A processing in FRα-positive cell lines

	IC_{50}, nmol/L (continuous exposure)			M9346A processing[b]		
Cell line	IMGN853	IMGN853+ M9346A[a]	*S*-methyl-DM4	Receptor density, antibody-binding sites/cell × 1,000	% Processed	pmol processed/ 10^6 cells
KB	0.10 ± 0.06	1.4 ± 0.5	0.03 ± 0.01	4,500 ± 640	29 ± 1	2.2 ± 0.4
Igrov	0.8 ± 0.3	10 ± 2	0.03 ± 0.01	1,300 ± 790	36 ± 1	0.75 ± 0.40
Jeg-3	0.9 ± 0.1	12 ± 5	0.03 ± 0.02	290 ± 130	57 ± 1	0.3 ± 0.1
Skov-3	7 ± 1	8 ± 1	0.06 ± 0.01	94 ± 13	30 ± 9	0.05 ± 0.01
Ovcar-3	3 ± 1	3.0 ± 0.6	0.02 ± 0.01	48 ± 14	24 ± 1	0.02 ± 0.01
HCC827	10 ± 0	10 ± 0	0.04 ± 0.01	58 ± 17	24 ± 7	0.02 ± 0.01
Ishikawa	1.0 ± 0.2	1.0 ± 0.4	0.05 ± 0.02	100 ± 8	28 ± 6	0.05 ± 0.01

NOTE: Data represent the mean ± SD of three independent experiments.
[a]M9346A was used at saturating concentration of 2 μmol/L.
[b]Assessed using ^{3}[H]-M9346A as described in Materials and Methods.

The number of FRα molecules on the surface of a cell is a key determinant of its sensitivity toward IMGN853

The cytotoxic activity of IMGN853 (continuous exposure) was evaluated on several FRα-positive cell lines that differed in FRα expression levels, while being similarly sensitive to the nonconjugated cell-permeable maytansinoid *S*-methyl-DM4 (Table 3). Three cell lines that expressed on the average 3×10^5 FRα per cell or higher were sensitive to IMGN853 in a FRα-selective manner, as indicated by the ability of an excess of unconjugated M9346A antibody to decrease the cytotoxic effect of the conjugate. The cytotoxicity of IMGN853 to four cell lines with FRα expression below 1×10^5 copies per cell was not decreased in the presence of an excess of M9346A.

In the presence of M9346A, the cytotoxicity of IMGN853 for the KB cell line after a continuous exposure was reduced 14-fold (the IC_{50} value increased from 0.1 nmol/L to 1.4 nmol/L), while the cytotoxicity of IMGN853 after a 4-hour exposure followed by 5-day culturing in conjugate-free medium was reduced 180-fold (Supplementary Fig. S5). The cytotoxicity of a maytansinoid conjugate with a nonreducible linker, M9346A-SMCC-DM1, was similar to that of IMGN853, and the cytotoxicity of a nontargeting human IgG1–SMCC–DM1 conjugate was similar to that of IMGN853 under blocking conditions (continuous exposure; Supplementary Fig. S6), suggesting that the nonspecific cytotoxicity of IMGN853 for KB cells was not a result of its reduction with the release of free maytansinoid in the medium, but possibly stemming from pinocytotic uptake of a conjugate by the cells. The seven cell lines reported in Table 3 differed in their sensitivity to IMGN853 under blocking conditions that may reflect different capacities for nonspecific uptake or metabolism of the conjugate.

The ability of the cell lines to process IMGN853 was also assessed as a possible determinant of their sensitivity to the conjugate. The intracellular processing of ^{3}[H]-IMGN853, in which tritium was incorporated into the C-20 methoxy group of the DM4, led to formation of three major catabolites, lysine-N^{ϵ}-sulfo-SPDB-DM4, DM4, and *S*-methyl-DM4 in KB cells (Supplementary Fig. S7). This result was similar to that previously reported for SPDB-linked DM4 conjugates (35). The extent of intracellular processing of ^{3}[H]-M9346A, where the antibody was labeled with the radioactive tracer *N*-succinimidyl-2,3-^{3}[H] propionate, was similar to that of ^{3}[H]-IMGN853 (Supplementary Fig. S8), suggesting that intracellular processing of the antibody and the conjugate both occur primarily through the lysosomal processing pathway, and that ^{3}[H]-M9346A could be used as a surrogate for IMGN853 processing. Assessment of the ^{3}[H]-M9346A processing in the seven cell lines evaluated for IMGN853 cytotoxicity demonstrated that the extent of antibody processing was similar in these cell lines (Table 3), suggesting that the total amount of active metabolite generated by processing IMGN853 in the cells was directly proportional to the antigen number on the cell surface, rather than to differences in the extent of conjugate processing.

IMGN853 is active in xenograft tumor models that express FRα at clinically relevant levels

Having observed a correlation between the level of cell-surface expression of FRα and specific sensitivity of cells to the cytotoxic effects of IMGN853 *in vitro*, it was important to assess the activity of IMGN853 in tumor xenograft models in mice that express FRα at levels representative of that in patients' tumors. Therefore, an IHC assay was developed with a dynamic range able to discern differing levels of FRα on patient tumor samples, in order to allow comparison with tumor xenograft samples. Analysis of ovarian and non-small cell lung tumor samples with this new assay revealed a wide variation in expression levels and incidence of FRα-positivity. Serous and endometrioid ovarian carcinomas and adenocarcinoma of the lung had the highest percentage of FRα positive tumors, consistent with previously reported data (6, 8). Most tumors of these subtypes were strongly positive, with 71%, 51%, and 59% having a score of $\geq$2 heterogeneous and homogeneous, respectively (Supplementary Table S6).

Levels of FRα expression on a panel of ovarian and non-small cell lung cancer cell line–derived xenografts grown in mice were also analyzed by the IHC method and compared with the levels detected in patient tumor tissues. FRα expression in Igrov-1, Ovcar-3, and OV-90 ovarian xenograft tumors was scored as 3 homogeneous, 3 heterogeneous, and 2 heterogeneous, respectively. These scores were similar to those of a majority of ovarian clinical tumor samples (Supplementary Table S6). FRα expression in non-small cell lung cancer xenografts of the cell line H2110 and of the LXFA737 patient-derived primary tumor xenograft scored as 3 homogeneous and 2 homogeneous, respectively, similar to the expression of FRα in a majority of non-small cell lung cancer samples tested (Supplementary Table S6). Xenograft samples from Skov-3 cells (which have low FRα level *in vitro*; see Table 3) scored negative for FRα expression by this IHC assay.

Antitumor activity of IMGN853 was assessed in mice bearing these xenografts (Fig. 3). The conjugate was found to be highly active in all FRα-positive xenograft models tested causing either complete or partial regressions (Ovcar-3, Igrov-1, H2110, and LXFA-737), or tumor growth delay (Ov-90), at the highest dose tested (a single administration of approximately 5 mg/kg). In the Ovcar-3 and Igrov-1 models, the conjugate was also active at a

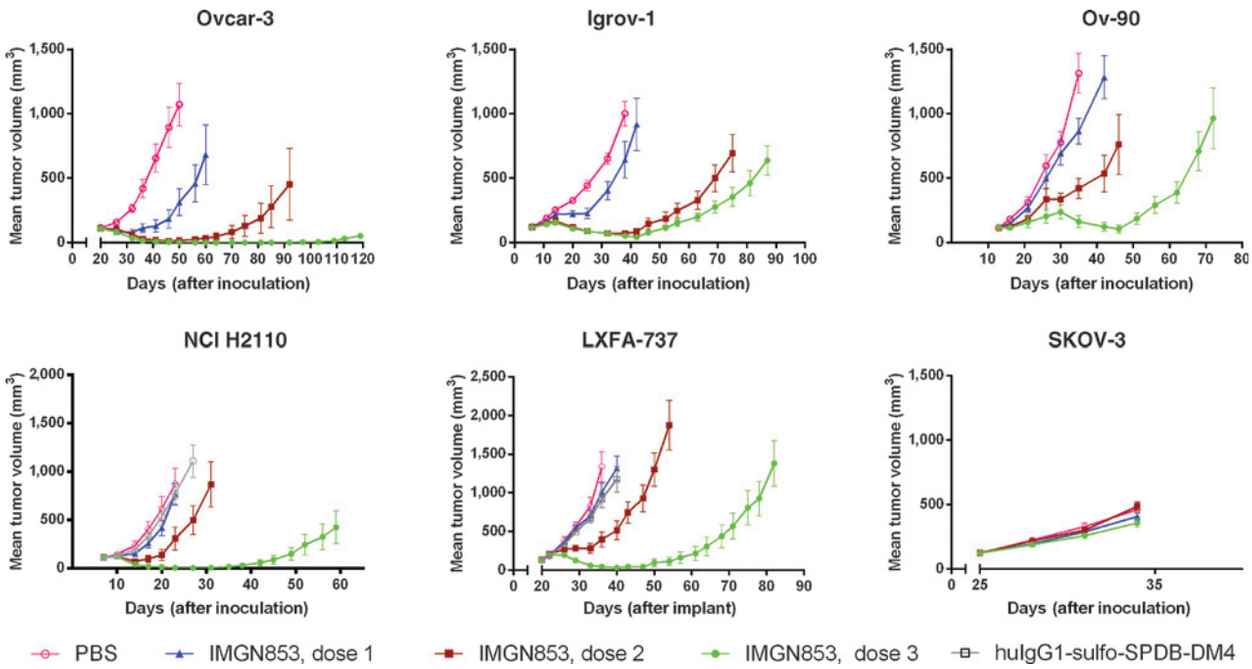

Figure 3.
IMGN853 activity against xenograft models derived from cell lines and a patient tumor. Mice bearing tumors derived from cell lines (Igrov-1, Ovcar-3, Ov-90, Skov-3, or H2110) or from a patient tumor (LXFA-737) received single intravenous injection of IMGN853, vehicle control PBS, or nontargeting huIgG1-sulfo-SPDB–DM4 conjugate. The conjugates were injected on day 7 (Igrov-1 and NCI-H2110), day 14 (Ov-90), day 20 (Ovcar-3, LXFA-737), or day 25 (Skov-3) after cell inoculation when the tumor volume reached about 130 mm^3. The xenografts were treated with IMGN853 at 1.2 ± 0.1 mg/kg (dose 1), 2.4 ± 0.2 mg/kg (dose 2), or 5.0 ± 0.3 mg/kg (dose 3), which is equivalent to 24 ± 3 μg/kg, 49 ± 2 μg/kg, and 98 ± 4 μg/kg conjugated maytansinoid per kg, respectively. Nontargeting huIgG1-sulfo-SPDB–DM4 conjugate was injected at 5.0 mg/kg (90 μg/kg conjugated maytansinoid). Some variability of the doses within each dose-group is the result of slightly different maytansinoid per antibody ratios of the tested conjugates; the exact doses for each group are listed in Supplementary Table S1. Mean tumor volumes in mm^3 versus time (in days) after cell inoculation are plotted.

lower single dose of 2.4 mg/kg. Multiple injections of the conjugate (2.8 mg/kg, weekly ×3) increased activity of IMGN853 causing more durable complete regression than that induced by a single injection (KB model; Supplementary Fig. S9). The conjugate was inactive against the FRα IHC–negative Skov-3 tumors, and a control conjugate of a nontargeting isotype-matched antibody was also inactive where tested (Fig. 3), demonstrating that IMGN853 activity is FRα-targeted. Thus, IMGN853 was highly active in ovarian and non-small cell lung cancer xenograft models that express FRα at clinically relevant levels. The conjugate was well tolerated at all tested doses. No toxicity was observed after IMGN853 treatment, as assessed by monitoring of clinical signs and body weight. In a separate experiment, the maximum-tolerated dose of IMGN853 in CD-1 mice was determined to be approximately 80 mg/kg.

Discussion

Ovarian cancer and endometrial cancer are the two most common gynecologic cancers, accounting in the United States for a combined 62,000 new cases and 23,000 deaths, and worldwide rates of 14.5 (incidence) and 5.8 (mortality) per 100,000 (42). Lung cancer, with more than 80% of it being non-small cell lung cancer, is the main cause of cancer-related deaths worldwide, mainly because of tobacco smoking and relatively poor efficacy of existing therapeutic approaches (43). Despite continuing advances in treating these cancers, there are still a large number of patients who progress to advanced metastatic disease, for which no curative treatment exists. Thus, there is an unmet medical need for these patients, and the effort is ongoing to develop novel therapeutic strategies, including the development of ADCs. FRα is an attractive therapeutic target for an ADC treatment for these cancers because, as the previous reports (3, 4, 6, 8) and this study show, it is highly and widely expressed on many types of ovarian and non-small cell lung cancer, while being absent or expressed only at low levels on most normal tissues.

IMGN853 is a conjugate of the M9346A antibody and the DM4 maytansinoid, which are joined via the disulfide-containing hydrophilic linker sulfo-SPDB. As reported here, the design of this conjugate, including selection of its antibody, linker, and maytansinoid components, was based on an experimental approach to optimize the antitumor activity of the ADC against FRα-expressing tumors. IMGN853 binds to FRα on the cell surface with high affinity, and then is internalized, degraded in the lysosomes, and active DM4 metabolites are released. These DM4 metabolites induce cell-cycle arrest and subsequent cell death. These metabolites are capable of diffusing into proximal tumor cells and killing them due to bystander cytotoxic activity (40). The bystander killing activity of a conjugate may be beneficial where its penetration into a solid tumor is limited and/or target expression among the tumor cells is heterogeneous. A similar thioether conjugate that was equally potent *in vitro*, but lacked the bystander cytotoxic activity, was much less efficient in eradicating xenograft tumors in mice, suggesting that bystander activity is an important

component of IMGN853 efficacy *in vivo*. The efficiency of processing of IMGN853 and generation of active DM4 metabolites was found to be similar in all tested FRα-positive cell lines, suggesting that the differences in their sensitivity to IMGN853 were not related to the conjugate processing. Among the anti-FRα conjugates tested with disulfide-containing linkers, the sulfo-SPDB-linked conjugate IMGN853 was the most active *in vivo*, while the SPP-linked conjugate was the least active. Our understanding of the factors that determine the antitumor activity of maytansinoid conjugates is not yet complete. At present, we can only speculate that this ranking of antitumor activity for the three conjugates may stem from the higher exposure of the intact sulfo-SPDB and SPDB conjugates compared with the SPP conjugate in tumor-bearing mice due to their more stable highly hindered disulfide bond, and, also, due to increased tumor retention of the conjugate with the more hydrophilic sulfo-SPDB linker compared with the less hydrophilic SPDB. Previously, we reported that huC242—SPDB–DM4 conjugate was retained longer in circulation of mice and had a greater antitumor activity on human tumor cell line xenografts in mice than huC242–SPP–DM1 (44). In addition, we found that sulfo-SPDB-linked conjugates were capable of eradicating P-glycoprotein–expressing multidrug resistant cells (45), which might be beneficial because some ovarian and non-small cell lung cancers express this protein (46).

Our data indicate that the expression of FRα on the cell surface is a key determinant of sensitivity of tumor cells to IMGN853, providing the rationale to further explore FRα expression in patient tumors as a candidate biomarker for IMGN853 activity. To this end, a clinical assay for semi-quantitative determination of FRα expression levels is currently under development, wherein FRα expression levels will be scored by the percentage of positively stained tumor cells at each of three staining intensities. Using an IHC assay capable of detecting differences in the levels of FRα expression in tumors, we identified xenograft tumor models that express FRα at levels similar to those found in ovarian and non-small cell lung cancer patient samples. IMGN853 was remarkably active in these models, with minimally effective doses on a mg/kg basis among the lowest reported for maytansinoid ADCs in preclinical studies. Our findings indicate that IMGN853 is a promising therapeutic candidate and support its clinical evaluation, currently under way, for treatment of FRα-expressing cancers (47).

Disclosure of Potential Conflicts of Interest

V.S. Goldmacher and J.M. Lambert have ownership interest (including patents) in ImmunoGen, Inc. No potential conflicts of interest were disclosed by the other authors.

Authors' Contributions

Design of the research: O. Ab, K.R. Whiteman, J. Pinkas, T. Chittenden
Development of methodology: O. Ab, K.R. Whiteman, X. Sun, R. Singh, V.S. Goldmacher
Acquisition of data (provided animals, acquired and managed patients, provided facilities, etc.): O. Ab, K.R. Whiteman, L.M. Bartle, X. Sun, A. LaBelle
Analysis and interpretation of data (e.g., statistical analysis, biostatistics, computational analysis): O. Ab, K.R. Whiteman, L.M. Bartle, A. LaBelle, J. Pinkas, V.S. Goldmacher
Writing, review, and/or revision of the manuscript: O. Ab, K.R. Whiteman, L.M. Bartle, A. LaBelle, G. Payne, R.J. Lutz, J. Pinkas, V.S. Goldmacher, T. Chittenden, J.M. Lambert
Administrative, technical, or material support (i.e., reporting or organizing data, constructing databases): D. Tavares
Study supervision: R.J. Lutz, J. Pinkas, T. Chittenden
Other (idea for humanized antibody): G. Payne
Other (discussing and advising on the research that led to the development of IMGN853): J.M. Lambert

The costs of publication of this article were defrayed in part by the payment of page charges. This article must therefore be hereby marked *advertisement* in accordance with 18 U.S.C. Section 1734 solely to indicate this fact.

Received December 26, 2014; revised April 10, 2015; accepted April 10, 2015; published OnlineFirst April 22, 2015.

References

1. Antony AC. The biological chemistry of folate receptors. Blood 1992;79:2807–20.
2. Matherly LH, Hou Z, Deng Y. Human reduced folate carrier: translation of basic biology to cancer etiology and therapy. Cancer Metastasis Rev 2007;26:111–28.
3. Franklin WA, Waintrub M, Edwards D, Christensen K, Prendegrast P, Woods J, et al. New anti-lung-cancer antibody cluster 12 reacts with human folate receptors present on adenocarcinoma. Int J Cancer Suppl 1994;8:89–95.
4. Miotti S, Canevari S, Menard S, Mezzanzanica D, Porro G, Pupa SM, et al. Characterization of human ovarian carcinoma-associated antigens defined by novel monoclonal antibodies with tumor-restricted specificity. Int J Cancer 1987;39:297–303.
5. O'Shannessy DJ, Somers EB, Maltzman J, Smale R, Fu YS. Folate receptor alpha (FRA) expression in breast cancer: identification of a new molecular subtype and association with triple negative disease. Springerplus 2012;1:22.
6. O'Shannessy DJ, Yu G, Smale R, Fu YS, Singhal S, Thiel RP, et al. Folate receptor alpha expression in lung cancer: diagnostic and prognostic significance. Oncotarget 2012;3:414–25.
7. Parker N, Turk MJ, Westrick E, Lewis JD, Low PS, Leamon CP. Folate receptor expression in carcinomas and normal tissues determined by a quantitative radioligand binding assay. Anal Biochem 2005;338:284–93.
8. Scorer P, Lawson N, Quinn A. A full immunohistochemical evaluation of a novel monoclonal antibody to folate receptor–alpha (FR-a). Novocastra J Histopathol, Reagents 2010;3:8–12.
9. Kalli KR, Oberg AL, Keeney GL, Christianson TJ, Low PS, Knutson KL, et al. Folate receptor alpha as a tumor target in epithelial ovarian cancer. Gynecol Oncol 2008;108:619–26.
10. Despierre E, Lambrechts S, Leunen K, Berteloot P, Neven P, Amant F, et al. Folate receptor alpha (FRA) expression remains unchanged in epithelial ovarian and endometrial cancer after chemotherapy. Gynecol Oncol 2013;130:192–9.
11. Lu Y, Sega E, Leamon CP, Low PS. Folate receptor-targeted immunotherapy of cancer: mechanism and therapeutic potential. Adv Drug Deliv Rev 2004;56:1161–76.
12. Marchetti C, Palaia I, Giorgini M, De Medici C, Iadarola R, Vertechy L, et al. Targeted drug delivery via folate receptors in recurrent ovarian cancer: a review. Onco Targets Ther 2014;7:1223–36.
13. Xia W, Low PS. Folate-targeted therapies for cancer. J Med Chem 2010;53:6811–24.
14. Pribble P, Edelman MJ. EC145: a novel targeted agent for adenocarcinoma of the lung. Expert Opin Investig Drugs 2012;21:755–61.
15. Reddy JA, Dorton R, Westrick E, Dawson A, Smith T, Xu LC, et al. Preclinical evaluation of EC145, a folate-vinca alkaloid conjugate. Cancer Res 2007;67:4434–42.
16. Serpe L, Gallicchio M, Canaparo R, Dosio F. Targeted treatment of folate receptor-positive platinum-resistant ovarian cancer and companion diagnostics, with specific focus on vintafolide and etarfolatide. Pharmgenomics Pers Med 2014;7:31–42.
17. Reddy JA, Dorton R, Dawson A, Vetzel M, Parker N, Nicoson JS, et al. *In vivo* structural activity and optimization studies of folate-tubulysin conjugates. Mol Pharm 2009;6:1518–25.

18. Reddy JA, Bloomfield A, Nelson M, Dorton R, Vetzel M, Leamon CP. Pre-clinical development of EC1456: a potent folate targeted tubulysin SMDC [abstract]. In: Proceedings of the 105th Annual Meeting of the American Association for Cancer Research; 2014 Apr 5–9; San Diego, CA. Philadelphia (PA): AACR; Cancer Res 2014;74(19 Suppl). Abstract nr 832.
19. Ebel W, Routhier EL, Foley B, Jacob S, McDonough JM, Patel RK, et al. Preclinical evaluation of MORAb-003, a humanized monoclonal antibody antagonizing folate receptor-alpha. Cancer Immun 2007;7:6.
20. Vergote I, Armstrong D, Scambia G, Fujiwara K, Gorbunova V, Schweizer C, et al. Phase 3 double-blind, placebo-controlled study of weekly farletuzumab with carboplatin/taxane in subjects with platinum-sensitive ovarian cancer in first relapse [abstract]. In: Proceedings of the European Society of Gynecological Oncology 18th International Meeting; 2013 Oct 19–22; Liverpool, United Kingdom; Int J Gynecol Cancer 2013;23(8 Suppl 1):11.
21. Lambert JM, Chari RV. Ado-trastuzumab Emtansine (T-DM1): an antibody–drug conjugate (ADC) for HER2-positive breast cancer. J Med Chem 2014;57:6949–64.
22. Pro B, Advani R, Brice P, Bartlett NL, Rosenblatt JD, Illidge T, et al. Brentuximab vedotin (SGN-35) in patients with relapsed or refractory systemic anaplastic large-cell lymphoma: results of a phase II study. J Clin Oncol 2012;30:2190–6.
23. Verma S, Miles D, Gianni L, Krop IE, Welslau M, Baselga J, et al. Trastuzumab emtansine for HER2-positive advanced breast cancer. N Engl J Med 2012;367:1783–91.
24. Younes A, Gopal AK, Smith SE, Ansell SM, Rosenblatt JD, Savage KJ, et al. Results of a pivotal phase II study of brentuximab vedotin for patients with relapsed or refractory Hodgkin's lymphoma. J Clin Oncol 2012;30:2183–9.
25. Lopus M, Oroudjev E, Wilson L, Wilhelm S, Widdison W, Chari R, et al. Maytansine and cellular metabolites of antibody–maytansinoid conjugates strongly suppress microtubule dynamics by binding to microtubules. Mol Cancer Ther 2010;9:2689–99.
26. Oroudjev E, Lopus M, Wilson L, Audette C, Provenzano C, Erickson H, et al. Maytansinoid-antibody conjugates induce mitotic arrest by suppressing microtubule dynamic instability. Mol Cancer Ther 2010;9:2700–13.
27. Kelly KR, Chanan-Khan A, Heffner LT, Somlo G, Siegel DS, Zimmerman T, et al. Indatuximab ravtansine (BT062) in combination with lenalidomide and low-dose dexamethasone in patients with relapsed and/or refractory multiple myeloma: clinical activity in patients already exposed to lenalidomide and bortezomib. Blood 2014;124:4736–4736.
28. Lambert JM. Drug-conjugated antibodies for the treatment of cancer. Br J Clin Pharmacol 2013;76:248–62.
29. Ribrag V, Dupuis J, Tilly H, Morschhauser F, Laine F, Houot R, et al. A dose-escalation study of SAR3419, an anti-CD19 antibody maytansinoid conjugate, administered by intravenous infusion once weekly in patients with relapsed/refractory B-cell non-Hodgkin lymphoma. Clin Cancer Res 2014;20:213–20.
30. Stathis A, Freedman AS, Flinn IW, Maddocks KJ, Weitman S, Berdeja JG, et al. A phase I study of IMGN529, an antibody–drug conjugate (ADC) targeting CD37, in adult patients with relapsed or refractory B-cell non-Hodgkin's lymphoma (NHL). Blood 2014;124:1760.
31. Widdison WC, Wilhelm SD, Cavanagh EE, Whiteman KR, Leece BA, Kovtun Y, et al. Semisynthetic maytansine analogues for the targeted treatment of cancer. J Med Chem 2006;49:4392–408.
32. Zhao RY, Wilhelm SD, Audette C, Jones G, Leece BA, Lazar AC, et al. Synthesis and evaluation of hydrophilic linkers for antibody–maytansinoid conjugates. J Med Chem 2011;54:3606–23.
33. Chari RV, Martell BA, Gross JL, Cook SB, Shah SA, Blattler WA, et al. Immunoconjugates containing novel maytansinoids: promising anticancer drugs. Cancer Res 1992;52:127–31.
34. Harlow E, Lane D. Antibodies: a laboratory manual. New York: Cold Spring Harbor Laboratory; 1988.
35. Erickson HK, Park PU, Widdison WC, Kovtun YV, Garrett LM, Hoffman K, et al. Antibody–maytansinoid conjugates are activated in targeted cancer cells by lysosomal degradation and linker-dependent intracellular processing. Cancer Res 2006;66:4426–33.
36. Kelemen LE. The role of folate receptor alpha in cancer development, progression and treatment: cause, consequence or innocent bystander? Int J Cancer 2006;119:243–50.
37. Coney LR, Tomassetti A, Carayannopoulos L, Frasca V, Kamen BA, Colnaghi MI, et al. Cloning of a tumor-associated antigen: MOv18 and MOv19 antibodies recognize a folate-binding protein. Cancer Res 1991;51:6125–32.
38. Figini M, Obici L, Mezzanzanica D, Griffiths A, Colnaghi MI, Winter G, et al. Panning phage antibody libraries on cells: isolation of human Fab fragments against ovarian carcinoma using guided selection. Cancer Res 1998;58:991–6.
39. Roguska MA, Pedersen JT, Keddy CA, Henry AH, Searle SJ, Lambert JM, et al. Humanization of murine monoclonal antibodies through variable domain resurfacing. Proc Natl Acad Sci U S A 1994;91:969–73.
40. Kovtun YV, Audette CA, Ye Y, Xie H, Ruberti MF, Phinney SJ, et al. Antibody–drug conjugates designed to eradicate tumors with homogeneous and heterogeneous expression of the target antigen. Cancer Res 2006;66:3214–21.
41. Polson AG, Williams M, Gray AM, Fuji RN, Poon KA, McBride J, et al. Anti-CD22-MCC-DM1: an antibody–drug conjugate with a stable linker for the treatment of non-Hodgkin's lymphoma. Leukemia 2010;24:1566–73.
42. Cramer DW. The epidemiology of endometrial and ovarian cancer. Hematol Oncol Clin North Am 2012;26:1–12.
43. Zalcman G, Bergot E, Lechapt E. Update on nonsmall cell lung cancer. Eur Respir Rev 2010;19:173–85.
44. Kellogg BA, Garrett L, Kovtun Y, Lai KC, Leece B, Miller M, et al. Disulfide-linked antibody–maytansinoid conjugates: optimization of *in vivo* activity by varying the steric hindrance at carbon atoms adjacent to the disulfide linkage. Bioconjug Chem 2011;22:717–27.
45. Kovtun Y, Jones G, Audette C, Mayo M, Leece B, Zhao R, et al. 235 Negatively-charged sulfonate group in linker improves potency of antibody–maytansinoid conjugates against multidrug-resistant cancer cells. Eur J Cancer Supplements 2010;8:76–7.
46. Leonard GD, Fojo T, Bates SE. The role of ABC transporters in clinical practice. Oncologist 2003;8:411–24.
47. Moore KN, Ponte J, LoRusso P, Birrer MJ, Bauer TM, Borghaei H, et al. Relationship of pharmacokinetics (PK), toxicity, and initial evidence of clinical activity with IMGN853, a folate receptor alpha (FRa) targeting antibody drug conjugate in patients (Pts) with epithelial ovarian cancer (EOC) and other FRa-positive solid tumors. J Clin Oncol 32:5s, 2014 (suppl; abstr 5571).